

An h -adaptive Time Domain Discontinuous Galerkin Method for Electromagnetics

Reza Abedi

Department of Mechanical Aerospace and Biomedical Engineering
University of Tennessee Space Institute (UTSI)
Tullahoma, TN, 37355, USA
rabedi@utsi.edu

Saba Mudaliar

Sensors Directorate
Air Force Research Laboratory, Wright-Patterson AFB
Dayton, OH 45433-7318, USA
saba.mudaliar@us.af.mil

Abstract—We present an h -adaptive time domain discontinuous Galerkin (TDDG) method for electromagnetics problem in which space and time are directly discretized by unstructured grids that satisfy a specific causality constraint. This enables a local and asynchronous solution procedure with arbitrary high and per element spacetime orders of elements. Our numerical results demonstrate that by using energy dissipation as an error indicator and local adaptive operations in spacetime we can significantly improve the efficiency of the method relative to nonadaptive solutions.

I. SPACETIME DISCONTINUOUS GALERKIN METHOD

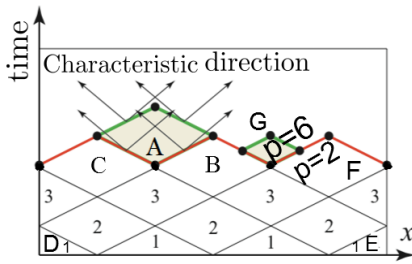


Fig. 1. Unstructured spacetime discretization used in the SDG method.

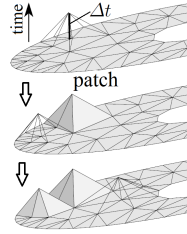


Fig. 2. Patch-by-patch solution procedure.

We present a *spacetime discontinuous Galerkin* (SDG) method that directly discretizes the spacetime using unstructured grids. Many exceptional properties of the method stem from the use of *causal meshes*. For example in the figure fig. 1 the solution of element A depends only on the solution of earlier elements B and C given that the red facets are causal (fastest waves shown in arrows only pass in one direction through the facet). The level-1 elements depend only on initial conditions and boundary conditions for the elements D and E. The level-1 element solutions can be computed locally and in parallel. Thus, causal SDG meshes enable asynchronous, element-by-element solutions with linear solution complexity.

In practice, we replace the individual elements in the $1d \times \text{time}$ with small clusters of simplicial elements called *patches*, where only the exterior patch facets need to be causal as shown in fig. 2 for clusters of tetrahedral elements in $2d \times \text{time}$. Using an advancing-front procedure, in each step the *Tent Pitcher* algorithm [1]–[3] advances in time a vertex in the *front mesh* to define a local front update; the causality

constraint limits the maximum time increment Δt at the vertex. We solve new patches as local problems and update the current front, until the entire spacetime analysis domain is solved.

II. EM FORMULATION

Given the lack of a natural metric in spacetime, we use the differential forms notation for our formulation. The standard basis for spacetime 1-forms is $\{dx^1, dx^2, dx^3, dt\}$. The *spacetime volume element* is the 4-form $\Omega := dx^1 \wedge dx^2 \wedge dx^3 \wedge dt$, where “ \wedge ” is the *exterior product operator* on forms. Using the Hodge star operator, the standard basis for 3-forms, $\{\star dx^j, \star dt\}$ is obtained as $\star dx^1 = dx^2 \wedge dx^3 \wedge dt$, $\star dx^2 = -dx^1 \wedge dx^3 \wedge dt$, $\star dx^3 = dx^1 \wedge dx^2 \wedge dt$ and $\star dt = -dx^1 \wedge dx^2 \wedge dx^3$. These satisfy $dx^i \wedge \star dx^j = \delta^i_j \Omega$, $dt \wedge \star dx^j = 0$, $dt \wedge \star dt = \Omega$ and $dx^i \wedge \star dt = 0$. Electric \mathbf{E} and magnetic \mathbf{H} fields are expressed as follows,

$$\mathbf{E} = E^1 dx_1 \wedge dt + E^2 dx_2 \wedge dt + E^3 dx_3 \wedge dt \quad (1a)$$

$$\mathbf{H} = H^1 dx_1 \wedge dt + H^2 dx_2 \wedge dt + H^3 dx_3 \wedge dt \quad (1b)$$

and electric \mathbf{D} and magnetic \mathbf{B} flux densities are given as,

$$\mathbf{D} = D_1 dx_2 \wedge dx_3 + D_2 dx_3 \wedge dx_1 + D_3 dx_1 \wedge dx_2 \quad (2a)$$

$$\mathbf{B} = B_1 dx_2 \wedge dx_3 + B_2 dx_3 \wedge dx_1 + B_3 dx_1 \wedge dx_2 \quad (2b)$$

By defining *spacetime electromagnetic flux density*,

$$\mathbf{M}^E := \mathbf{D} - \mathbf{H} \quad \mathbf{M}^H := \mathbf{B} + \mathbf{E} \quad (3)$$

all Maxwell’s equations can be written in the following form,

$$d\mathbf{M} + \mathbf{R}_M = 0 \quad (4)$$

where the *spacetime electromagnetic source terms* $\mathbf{R}_M = \mathbf{J} + \rho$ combine electromagnetic current density $\mathbf{J} = [\mathbf{J}^E \ \mathbf{J}^H]^T$ and charge density $\rho = [\rho^E \ \rho^H]^T$ forms. ¹ The expanded form of (4) is,

$$\left(\dot{\mathbf{D}} + \mathbf{J}^E - \nabla \times \mathbf{H} \right) \star d\mathbf{x} - (\nabla \cdot \mathbf{D} - \rho^E) \star dt = 0 \quad (5a)$$

$$\left(\dot{\mathbf{B}} + \mathbf{J}^H + \nabla \times \mathbf{E} \right) \star d\mathbf{x} - (\nabla \cdot \mathbf{B} - \rho^H) \star dt = 0 \quad (5b)$$

¹In general $\mathbf{J}^H = 0$ and $\rho^H = 0$ but this generality allows formulation of certain artificial media used in computational electromagnetics.

where the terms multiplying $\mathbf{dx} = \mathbf{e}_i dx^i$ in (5a) and (5b) are Ampère's law with Maxwell addition and Faraday law of induction, respectively, and the terms multiplying $\star dt$ are Gauss laws of electric and magnetic fields.

To obtain the discrete electromagnetic fields $\mathbf{U}^h := [\mathbf{E}^h \ \mathbf{H}^h]^T$ for each element \mathcal{Q} (e.g., elements A to G in fig. 1), the weighted residual statement for Ampère and Faraday laws is formed by requiring that for all weight functions $\hat{\mathbf{U}} = [\hat{\mathbf{E}} \ \hat{\mathbf{H}}]^T$ in discrete space,

$$-\int_{\mathcal{Q}} \mathbf{i} \hat{\mathbf{U}} \wedge (d\mathbf{M}^h + \mathbf{R}_M^h) + \int_{\partial\mathcal{Q}} \mathbf{i} \hat{\mathbf{U}} \wedge (\mathbf{M}^* - \mathbf{M}) = \mathbf{0} \quad (6)$$

where \mathbf{M}^* are the numerical fluxes on the spacetime boundary of an element $\partial\mathcal{Q}$ that are obtained by the solution to a local Riemann problem herein.

The expanded form of discrete weak statement, which is used in our numerical implementation, is obtained by the application of Stokes theorem on (6),

$$\begin{aligned} & \int_{\partial\mathcal{Q}} \left\{ \left(\hat{\mathbf{E}} \cdot \mathbf{D}^* + \hat{\mathbf{H}} \cdot \mathbf{B}^* \right) \star dt + \left(\hat{\mathbf{E}} \times \mathbf{H}^* - \hat{\mathbf{H}} \times \mathbf{E}^* \right) \star d\mathbf{x} \right\} \\ & + \int_{\mathcal{Q}} \left\{ \left(-\hat{\mathbf{E}} \cdot \mathbf{D}^h - \nabla \times \hat{\mathbf{E}} \cdot \mathbf{H}^h + \hat{\mathbf{E}} \cdot \mathbf{J}^{hE} \right) \right. \\ & \left. + \left(-\hat{\mathbf{H}} \cdot \mathbf{B}^h + \nabla \times \hat{\mathbf{H}} \cdot \mathbf{E}^h + \hat{\mathbf{H}} \cdot \mathbf{J}^{hH} \right) \right\} \Omega = 0 \end{aligned} \quad (7)$$

III. h -ADAPTIVE METHOD

The spacetime electromagnetic energy flux $\mathbf{N} := \mathbf{u} + \mathbf{S}$ combines *electromagnetic energy density form* $\mathbf{u} = \frac{1}{2}(\mathbf{E} \cdot \mathbf{D} + \mathbf{H} \cdot \mathbf{B}) \star dt$ and Poynting form $\mathbf{S} := \mathbf{E} \wedge \mathbf{H} = \mathbf{E} \times \mathbf{H} \star dx$. In discrete setting \mathbf{N} is expressed in terms of target fluxes for \mathbf{U}^* . Unlike continuum setting where energy is balanced, our discrete method is dissipative, i.e., it can be shown that the numerical energy dissipation for an element \mathcal{Q} is nonnegative,

$$\Delta_{\mathcal{Q}} := - \left[\int_{\partial\mathcal{Q}} \mathbf{N}(\mathbf{U}^*) + \int_{\mathcal{Q}} \mathbf{R}_N \right] \geq 0 \quad (8)$$

where $\mathbf{R}_N := (\mathbf{E} \cdot \mathbf{J}^E + \mathbf{H} \cdot \mathbf{J}^H) \Omega$ is the *energy balance source term*.

Let $\bar{\Delta} > \underline{\Delta}$ be two adaptivity energy tolerances. An element calls for local front refinement if $\Delta_{\mathcal{D}} > \bar{\Delta}$. The next time Tent-Pitcher [1] resumes front elements are refined and a smaller element is generated. For example, in fig. 1 a refinement call for an original element of the size of element A on top of elements B and F results in a smaller element G the next time a patch is erected there. If needed the spacetime order of element can also be increased (p -enrichment) as shown, an option not exercised herein. On the other hand, if $\Delta_{\mathcal{D}} < \underline{\Delta}$ the element is coarsenable and through spacetime mesh adaptive operations [1], [3], the front mesh is coarsened when possible and larger spacetime elements are created afterwards.

IV. NUMERICAL RESULTS

We solved a Transverse Electric (TE) wave scattering problem with initial condition $H_3(x_1, x_2) = \cos(\frac{\pi}{2} \frac{x_1}{l}) \cos(\frac{\pi}{2} \frac{x_2}{l})$ for $|x_1|, |x_2| \leq l$ in the red square with $l = 0.0625$, and zero E_1, E_2, E_3 elsewhere. The electrical permittivity and permeability for the interior (i) and exterior (e) regions, cf. fig. 3 are $\epsilon_i = 1, \mu_i = 1$ and $\epsilon_o = 10, \mu_o = 1$, respectively.

a/na	h_{\min}	h_{ave}	time (hour)	Δ	# patches
a	$9.77e-4$	0.0303	72.23	$1.08e-4$	$2.77e6$
na	0.0474	0.0747	14.17	$1.37e-3$	$4.73e5$
na	0.0275	0.04296	92.49	$8.04e-4$	$2.55e6$
na	0.0134	0.0236	541.0	$1.94e-4$	$1.56e7$

TABLE I
COMPARISON OF ADAPTIVE (FIRST ROW) AND NONADAPTIVE RUNS.

Table I compares minimum and average element sizes (h_{\min} , h_{ave}), simulation time, total energy dissipation $\Delta = \sum_{\mathcal{Q}} \Delta_{\mathcal{Q}}$, and number of patches between one adaptive run (first row) and three nonadaptive simulations with successively finer grids. As evident, the adaptive run

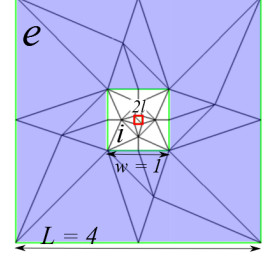


Fig. 3. Initial mesh and schematic of TE numerical example.

achieves a smaller error than even the finest nonadaptive run at substantially lower simulation time. Note that the adaptive run starts with only 46 elements on the spatial front, cf. fig. 3, and this number increases as wave fronts form and propagate. In contrast, for nonadaptive runs the number of elements on the spatial front is fixed and ranges from 8256 (coarsest run) to 83071 (finest run). Figure fig. 4 presents a sequence of H_3 solution for the adaptive run and fig. 5 depicts the cleaner resolution of wave front for the adaptive simulation.

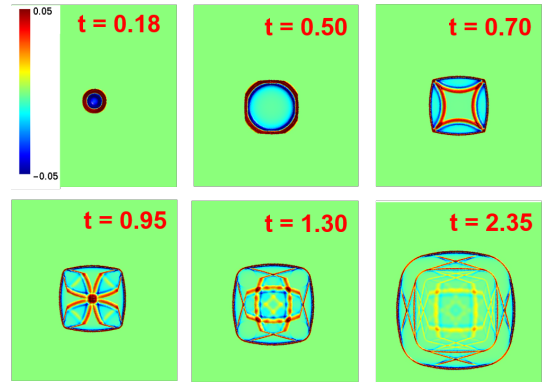


Fig. 4. Sequence of H_3 mapped to color for the adaptive run.

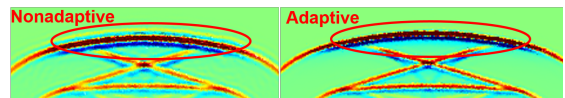


Fig. 5. Comparison of adaptive and second nonadaptive runs at $t = 2.35$.

REFERENCES

- [1] R. Abedi, S.-H. Chung, J. Erickson, Y. Fan, M. Garland, D. Guoy, R. Haber, J. M. Sullivan, S. Thite, and Y. Zhou, "Spacetime meshing with adaptive refinement and coarsening," in *Proceedings of the Twentieth Annual Symposium on Computational Geometry*, ser. SCG '04. ACM, June 9-11 2004, pp. 300-309.
- [2] S. Thite, "A unified algorithm for adaptive spacetime meshing with nonlocal cone constraints," in *Proc. 21st European Workshop Comput. Geom. (EWCG)*, Eindhoven, Netherlands, 2005, pp. 1-4.
- [3] R. Abedi, R. B. Haber, S. Thite, and J. Erickson, "An h -adaptive spacetime-discontinuous Galerkin method for linearized elastodynamics," *Revue Européenne de Mécanique Numérique (European Journal of Computational Mechanics)*, vol. 15, no. 6, pp. 619-642, 2006.